American Mineralogist, Volume 59, pages 536–548, 1974

Phase Relations of Titan-Acmite in the System Na_2O-Fe_2O_3-Al_2O_3-TiO_2-SiO_2 at 1000 Bars Total Water Pressure

MARTIN F. J. FLOWER
Institut für Mineralogie der Ruhr-Universität,
463 Bochum, West Germany

Abstract

Phase relations in the two pseudobinary joins $NaFeSi_2O_6$–$NaTiFeSiO_6$ (acmite-'tf') and $NaFeSi_2O_6$–$NaTiAlSiO_6$ (acmite-'tx') in the system Na_2O–Fe_2O_3–Al_2O_3–TiO_2–SiO_2 have been studied at 1000 bars P_{H_2O}, and oxygen fugacities controlled by the Mn_2O_3–Mn_3O_4 buffer. At 700°C binary pyroxene solid solutions containing up to 28 mole percent tf and 15 mole percent tx, respectively, are stable, although miscibility is greatly reduced at the Ni–NiO buffer. The solid solution is interpreted in terms of the coupled substitutions $TiFe^{3+} = Fe^{3+}Si$ in tf-pyroxenes and $TiAl = Fe^{3+}Si$ in tx-pyroxenes. Stable subsolidus phases in the acmite-tf join are pyroxene$_{ss}$ + hematite + freudenbergite (a non-stoichiometric member of the series $Na_2O \cdot Fe_2O_3 \cdot (6 + x)TiO_2$). In the acmite-tx join, however, nepheline is an additional subsolidus phase; the extent to which hematite is attributable to vapor-phase leaching is uncertain. The pyroxene solid solutions melt incongruently over intervals of ~100°C (for the most tf-rich pyroxene) and ~130°C (for the most tx-rich pyroxene), the respective solidi being at 775(±10)°C and 745(±10)°C. In tf- and tx-rich parts of the joins, pseudobrookite has a field of stability above 850(±10)°C and 790(±10)°C respectively, coinciding with final disappearance of pyroxene$_{ss}$. High temperature favors incorporation of tf, and probably tx, whereas entry of titanium into acmite is greatest at high oxygen fugacities. Zoned aegirines from a Gran Canaria ignimbrite (silica-oversaturated) and Tenerife lavas (silica-undersaturated) show strong enrichment in tf (approaching 25 mole percent), those from Tenerife also showing significant contents of tx (up to 8 mole percent). In nepheline-syenites from the Katzenbuckel (Odenwald), freudenbergite has been found in association with titaniferous aegirine, hematite, nepheline, and alkali feldspar (Frenzel, 1961). These occurrences of titan-pyroxene indicate that conditions of extremely high oxygen fugacity prevailed during the late-stage consolidation and/or alteration of such peralkaline rocks.

Introduction

It has generally been accepted that pyroxenes evolving within fractionating series of alkalic magma have followed a compositional trend of the type: augite—soda-augite—aegirine-augite—aegirine, with a possible divergence from soda-augite to soda-hedenbergite. For many examples of such trends the titanium contents of early augites are high (up to 6 percent TiO_2) but decline as the later acmitic pyroxenes are formed, *e.g.*, Morotu (Yagi, 1953), Iki (Aoki, 1959; 1964), Atumi dolerite (Kushiro, 1964) and Takakusayama (Tiba, 1966). In other series such as the Miocene lavas and ignimbrites of Gran Canaria (Schmincke and Frisch, in preparation), the Las Canadas lavas of Tenerife (Scott, 1970), and the nepheline-syenites of Katzenbuckel (Frenzel, personal communication), titanium contents in pyroxene increase dramatically in the latest (peralkaline) stages of magma evolution. In calcium-bearing pyroxenes titanium occurs to variable extents as $CaTiAl_2O_6$ (Yagi and Onuma, 1967), $CaMgTi_2O_6$ (Barth, 1931), and $CaTiFe^{3+}{}_2O_6$ (Huckenholz, 1969); however, the sharp increase of titanium with increasing sodium and ferric iron in aegirine must be explained in terms of sodium-bearing end-member species.

Verhoogen's (1962) view that partition of titanium between silicate and oxide phases is very sensitive to oxygen fugacity (f_{O_2}) with a high f_{O_2} generally favoring its incorporation by silicates, at least below the temperature of pseudobrookite stability, is substantiated by the occurrence of titan-aegirines[1] in highly oxidized natural mineral assemblages. Fluctuations of f_{O_2} during crystallization of evolved, and even relatively primitive, magmas is a well-recognized phenomenon, and there is evidence of considerable variation between early-formed and later-formed crystallization products. An excellent example is the

[1] The term 'titan-aegirine' (Schmincke, 1969; Schmincke and Frisch, in preparation) is proposed for aegirine with more than 0.1 atoms of titanium per formula unit.

Picture Gorge Basalt (Lindsley and Haggerty, 1970) where the effects of introduced water and atmospheric oxygen into joint selvages during late-stage crystallization are reflected by the presence of pseudobrookite ($Fe^{3+}TiO_5$) in the selvage, and a decrease of mean magnetite oxidation index into the host rock until such minerals as fayalite ($Fe^{2+}{}_2SiO_4$) and aenigmatite ($Na_2Fe^{2+}{}_5TiSi_6O_{20}$) are encountered.

The present experimental study of such problems began with an investigation of two joins between acmite and the theoretical end-members $NaTiFe^{3+}SiO_6$ (tf) and $NaTiAlSiO_6$ (tx). The acmite-tf join is contained by the four-oxide component system Na_2O-Fe_2O_3-TiO_2-SiO_2, (NFTS), shown schematically in Figure 1. The acmite-tx join is contained by the five-oxide component system Na_2O-Fe_2O_3-Al_2O_3-TiO_2-SiO_2 and may be represented graphically in terms of the four components $NaFe^{3+}SiO_4$-$NaAlSiO_4$-TiO_2-SiO_2 (Fig. 2). This work is essentially a study of subsolidus relations in these joins, particularly of pyroxene miscibility. Attention has been confined to phase relations at high f_{O_2} levels at total water pressures of 1000 bars.

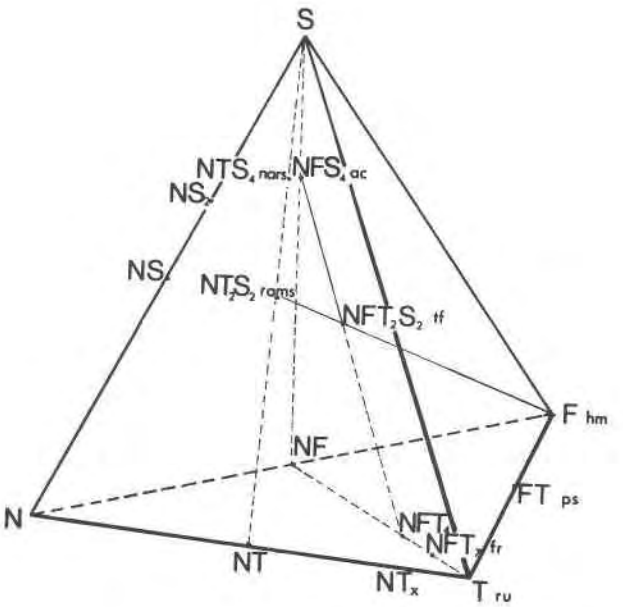

FIG. 1. The quaternary system Na_2O–Fe_2O_3–TiO_2–SiO_2 (NFTS) indicating relations of the join acmite-$NaFeTiSiO_6$ (ac-tf) and the phases narsarsukite (nars), ramsayite (rams), hematite (hm), pseudobrookite (ps), freudenbergite (fr) and rutile (ru). The range of sodium titanates (NT–NT_x) is also shown.

Previous Work on Acmite

Acmite has been the subject of extensive experimental investigation. Bailey (1969) confirmed that it is stable between 2 and 5 kbar within the range of f_{O_2} defined by the hematite-magnetite and quartz-fayalite-magnetite buffers, and Gilbert (1969) has shown that acmite melts incongruently to hematite + liquid up to at least 45 kbar. Complete miscibility probably exists between acmite and jadeite at 40 kbar (Gilbert, 1967), and has been confirmed between acmite and diopside at 1 atmosphere (Yagi, 1966) and at 10 kbar (Cassie, 1970). There is probably substantial miscibility between acmite and hedenbergite (Carmichael, 1962; Nolan, 1969), and possibly also with ferrosilite (Yagi, 1966). Recently, Popp and Gilbert (1972) studied the join $NaFe^{3+}Si_3O_8$-$NaAlSi_3O_8$ at 4 kbar to determine the position of the curve separating the stability fields of clinopyroxene + albite + quartz from clinopyroxene + quartz. At f_{O_2} approximating to the Ni-NiO buffer at 500°C they found 5–6 mole percent $NaAlSi_2O_6$ solid solution in acmitic pyroxenes.

Experimental Procedure

Starting gels were prepared by the method of Hamilton and Henderson (1968) for the 'end-member' compositions acmite ($NaFeSi_2O_6$), nepheline ($NaAlSiO_4$), 'tf' ($NaTiFeSiO_6$), 'tx' ($NaTiAlSiO_6$), ramsayite ($Na_2Ti_2Si_2O_9$), and for intermediate compositions on the joins acmite-tf and acmite-tx. Several compositions were prepared by mixing gels (see Tables 1 and 2).

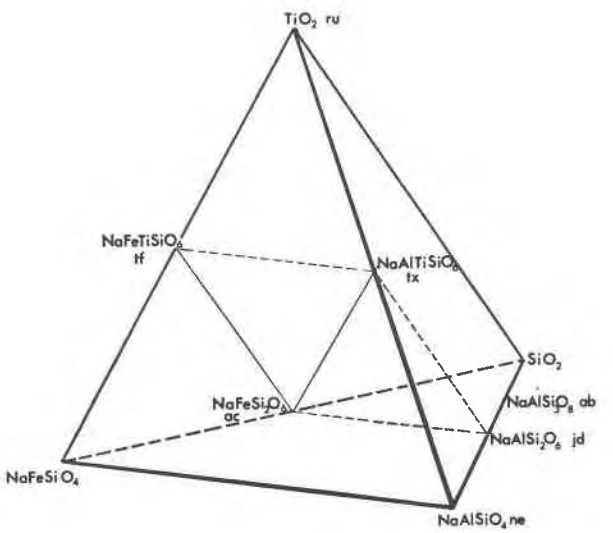

FIG. 2. The pseudoquaternary system $NaFeSiO_4$–$NaAlSiO_4$–TiO_2–SiO_2 showing relations of the joins acmite-tf, and acmite-tx. Note that the joins acmite-jadeite and jadeite-tx are coplanar.

TABLE 1. Selected Results from Experiments on the Join $NaFeSi_2O_6$ – $NaTiFeSiO_6$ for P_{H_2O} = 1000 Bars (±50)†

Starting Material	Compn.	Wt.% H_2O	Temp. (°C±10)	Time (hours)	Condensed Phase Assemblage
		Oxygen Buffer: Mn_2O_3-Mn_3O_4			
gel	ac_{100}	10	700	192	px
gel	tf_{20}	10	700	192	px
gel	tf_{20}	3-4	800	72	px+hm+gl
gel	tf_{40}	3-4	700	96	px+fr+hm
gel	tf_{40}	3-4	800	68	px+fr+hm+gl
gel	tf_{100}	3-4	770	118	px+fr+hm+(NS)
gel	tf_{20}	3-4	775	112	px
gel	tf_{30}	3-4	775	112	px
gel	tf_{30}	3-4	800	112	px+hm+gl
gel	tf_{40}	3-4	775	112	px+fr+(hm)
gel	tf_{10}	3-4	775	84	px
gel	tf_{10}	3-4	700	184	px
ac+rms+hm	tf_{100}	5	700	130	px+fr+hm+(NS)
ac+rms+hm	tf_{30}	5	700	124	px+fr
ac+rms+hm	tf_{50}	5	700	124	px+fr+hm
gel	tf_{20}	3-4	900	23	(px)+hm+gl
gel	tf_{40}	3-4	900	23	hm+gl
gel	tf_{100}	3-4	900	23	fr+(ps)+gl
		Oxygen Buffer: Ni-NiO			
gel	tf_{100}	3-4	700	330	px+fr+ilm+(NS?)
gel	tf_{10}	3-4	700	330	px+(ilm)
gel	tf_{30}	3-4	700	330	px+fr+ilm+(NS?)
gel	tf_{50}	3-4	700	330	px+fr+ilm+(NS)
		Oxygen Buffer: Mn_2O_3-Mn_3O_4			
gel	tf_{10}	3-4	790	136	px
gel	tf_{10}	3-4	800	96	px+hm+(gl)
gel	tf_{10}	3-4	850	72	px+hm+gl
gel	tf_{20}	3-4	790	72	px+hm+(gl)
gel	tf_{50}	3-4	800	72	px+fr+hm+gl
gel	tf_{50}	3-4	830	96	px+fr+hm+gl
gel	tf_{10}	5	900	18	(px)+hm+gl
gel	tf_{30}	5	900	18	hm+gl
gel	tf_{45}**	5	900	18	ps+hm+gl
gel	tf_{50}	5	900	18	ps+fr+gl
gel	tf_{40}	3-4	850	70	hm+(fr)+(ps)+gl
gel	tf_{50}	3-4	850	70	hm+fr+ps+gl
gel	tf_{35}**	3-4	775	112	px+(hm?)
gel	tf_{30}	3-4	750	76	px
gel	tf_{35}**	3-4	750	76	px+fr
gel	tf_{30}	3-4	720	160	px
gel	tf_{35}**	3-4	800	56	px+hm+gl
gel	tf_{45}**	3-4	800	56	px+fr+hm+gl
gel	tf_{30}	3-4	850	48	px+hm+gl
gel	tf_{35}**	3-4	850	48	(px)+hm+gl

†*A vapour phase is inferred in all runs.*

Abbreviations used:
ac acmite, fr freudenbergite, gl glass, hm hematite, tf $NaTiFeSiO_6$, ilm ilmenite, mt magnetite, ne nepheline, NS sodium metasilicate, ps pseudobrookite, px pyroxene, rms ramsayite, ru rutile

**Previous run products.*
***Gel mixes.*

TABLE 1, Continued

Starting Material	Compn.	Wt.% H_2O	Temp. (°C±10)	Time (hours)	Condensed Phase Assemblage
px+hm+gl*	tf_{20}	5	700	164	px
px+hm+gl*	tf_{20}	5	775	160	px+(hm)
px+hm+gl*	tf_{20}	5	800	98	px+hm+gl
px+hm+gl*	tf_{30}	5	750	128	px
px+hm+gl*	tf_{30}	5	775	124	px+(hm)
px+hm+gl*	tf_{30}	5	700	168	px+fr
px+hm+fr+NS*	tf_{40}	5	775	160	px+fr+hm
px+fr+ilm+NS*	tf_{30}	5	750	50	px
gel	tf_{35}**	3-4	840	72	px+hm+gl
gel	tf_{35}**	3-4	700	168	px+fr
gel	tf_{45}**	3-4	840	70	px+fr+hm+gl
gel	tf_{45}**	3-4	750	80	px+fr+hm
		Oxygen Buffer: Fe_3O_4-Fe_2O_3			
gel	ac_{100}	5	890	8	px+hm+mt+(gl)
gel	ac_{100}	5	880	8	px
		Oxygen Buffer: Mn_2O_3-Mn_3O_4			
gel	ac_{100}	5	900	23	px

Required proportions of the constituent elements were introduced into 65 percent nitric acid as follows: (1) Na as Na_2CO_3 (Merck analytical grade), dried at 350°C; (2) Al as aluminum metal (Schuchardt analytical grade), dried at 110°C; (3) Fe as iron filings (Merck analytical grade), under ice-cooling to prevent hydrolysis and precipitation of iron hydroxide, this stage being *preceded* by evaporation to near-dryness; (4) Ti as a previously standardized solution of $TiO_2 \cdot H_2O$ in 65 percent nitric acid, also under ice-cooling to avoid precipitation of TiO_2; $TiO_2 \cdot H_2O$ was precipitated from a saturated aqueous solution of titanyl sulfate (Riedel de Haën analytical grade) by addition of 25 percent ammonia solution. The precipitate was washed with distilled water by repeated centrifuging and the TiO_2 of the resulting acid solution was determined gravimetrically.

To check the accuracy of the gel preparation technique, four gels were analyzed for Na_2O, TiO_2 (colorimetrically), and H_2O, the results for Na_2O and TiO_2 (corrected to a water-free basis) being as follows:

gel composition	wt percent (Na_2O)		wt percent (TiO_2)	
	obs	calc	obs	calc
$ac_{90}tx_{10}$	13.0	13.5	3.4	3.5
$ac_{60}tx_{40}$	13.6	13.6	13.8	14.0
$ac_{80}tf_{20}$	13.0	13.2	7.0	6.8
$ac_{60}tf_{40}$	12.8	13.0	13.0	13.3

TABLE 2. Selected Results from Experiments on the Join $NaFeSi_2O_6$ – $NaTiAlSiO_6$ for P_{H_2O} = 1000 Bars (±50)†

Compn. Mole % tx	Wt. % H_2O	Temp. (°C±10)	Time (Hours)	Condensed Phase Assemblage
Oxygen Buffer: Mn_2O_3-Mn_3O_4; Starting material: gel				
10	10	700	72	px+?
20	5	700	72	px+ne
30	10	700	168	px+ne+fr+hm+?
40	10	700	170	px+ne+fr+hm+NS
40	10	750	150	px+ne+fr+hm+NS+(gl)
50	3-4	700	144	px+ne+fr+hm
30	3-4	750	144	px+ne+fr+hm+(gl)
10	3-4	800	82	px+hm+gl
30	3-4	800	82	(px)+ne+hm+gl
40	3-4	800	70	ne+(fr)+hm+gl
50	3-4	800	72	ne+hm+ps+fr+gl
50	3-4	750	120	px+ne+fr+hm+(gl)
50	3-4	775	120	px+ne+fr+hm+gl
Unbuffered; Starting material: gel				
100	20	700	164	ru+ne+(NS)?
Oxygen Buffer: Mn_2O_3-Mn_3O_4; Starting material: gel				
40	3-4	775	120	px+ne+fr+hm+gl
20	3-4	800	110	px+hm+gl
20	3-4	750	120	px+ne+hm+gl
35	3-4	750	124	px+ne+fr+hm+(gl)
45**	3-4	750	124	px+ne+fr+hm+(gl)
35**	3-4	800	76	ne+hm+gl
45**	3-4	800	76	ne+hm+fr+gl
15**	3-4	850	56	px+hm+gl
20	3-4	850	56	hm+gl
30	3-4	780	97	px+ne+(fr)+hm+gl
48**	3-4	780	97	px+ne+hm+fr+gl
48**	3-4	720	143	px+ne+fr+hm
48**	3-4	800	84	ne+fr+hm+gl
15**	3-4	800	82	px+hm+gl
15**	3-4	775	98	px+hm+gl
15**	3-4	750	98	px+hm+(gl?)
50	3-4	790	98	(px)+ne+fr+hm+gl
25**	3-4	800	68	(px)+(ne)+hm+gl
20	3-4	775	76	px+hm+gl
15**	2	740	120	px
15**	2	700	121	px
25**	3-4	750	122	px+ne+fr+hm+(gl)
25**	3-4	740	144	px+ne+(fr)+hm
25**	3-4	700	163	px+ne+(fr)+hm
5**	3-4	800	56	px+hm+(gl)
Oxygen Buffer: Mn_2O_3-Mn_3O_4; Starting material: ac+ne+ru				
20	10	700	668	px+ne+?
50	10	700	668	px+ne+fr+hm
Oxygen Buffer: Mn_2O_3-Mn_3O_4; Starting material: gel				
20	4	900	19	hm+gl
50	4	900	19	px+hm+gl
5**	4	900	19	px+hm+gl
40	4	900	18	hm+gl
45**	4	900	18	(ps)+hm+gl
30	4	900	24	hm+gl
10	4	900	19	hm+gl
*Oxygen Buffer: Mn_2O_3-Mn_3O_4; Starting material: px+hm+gl**				
20	4	740	122	px+ne+(hm)
20	5	750	102	px+ne+hm+(gl)
*Oxygen Buffer: Mn_2O_3-Mn_3O_4; Starting material: hm+ne+gl+(px)**				
30	5	780	95	px+ne+fr+hm+gl
30	5	750	112	px+ne+fr+hm+(gl)

†*A vapour phase is inferred to have been present in all runs. See Table 1, † footnote for abbreviations used.*
**Previous run products.*
***Gel mixes.*

TABLE 2, Continued

Compn. Mole % tx	Wt. % H_2O	Temp. (°C±10)	Time (Hours)	Condensed Phase Assemblage
*Oxygen Buffer: Mn_2O_3-Mn_3O_4; Starting material: hm+gl**				
40	5	700	68	px+ne+fr+hm
40	5	790	76	(px)+ne+(fr)+hm+gl
*Oxygen Buffer: Mn_2O_3-Mn_3O_4; Starting material: px+hm+gl**				
5**	5	750	138	px
5**	5	780	48	px
Oxygen Buffer: Mn_2O_3-Mn_3O_4; Starting material: gel				
25**	4	775	52	px+ne+hm+gl
25**	4	810	36	px+hm+gl
30	4	810	36	hm+(ne)+gl
40	4	810	36	hm+ne+gl
45**	4	810	36	hm+ne+gl
50	4	810	36	hm+ne+(ps)+gl+(fr)
10	4	750	48	px

Additional starting compositions were prepared as mixes in required proportions (described later) of the following synthetic crystalline phases: acmite, ramsayite, nepheline, hematite, and rutile. The first three had each been synthesized hydrothermally from gels at 1000 bars and 750°C, during runs of about one week's duration, while hematite and rutile were obtained as laboratory reagents (Merck, analytical grade, and Kronos, reagent grade, respectively). All mixes were ground under acetone for 3/4 hour.

Cold seal hydrothermal pressure vessels were utilized for experiments up to 850°C at 1000 bars pressure. Pressure measurements were accurate within ±50 bars, and temperature control, by chrome-alumel thermocouple, is believed to be within 10°C of the given temperature. Experiments at temperatures of 900°C were run in an internally heated pressure vessel modified by F. Seifert from the design of Yoder (1950). Pressure was read from a Bourdon gauge and was accurate within ±5 bars. Temperatures were read from Pt – $Pt_{90}Rh_{10}$ thermocouples and kept constant to within ±5°C. In most experiments f_{O_2} was buffered by the assemblage Mn_2O_3-Mn_3O_4 (bixbyite-hausmannite) using the double-tube technique of Eugster and Wones (1962). The sample plus H_2O was encapsulated in a sealed Pt or Ag/Pd tube, around which the buffering assemblage (in most cases a 9:1 ratio of Mn_2O_3 to Mn_3O_4 plus about 15 wt percent H_2O) was enclosed by a sealed outer Au tube. A few synthesis experiments were also conducted using the Ni-NiO and Fe_3O_4-Fe_2O_3 buffer assemblages. The oxidation conditions at the Mn_2O_3-Mn_3O_4 buffer may be expressed by the equation:

$$\log f_{O_2} = 7.34 - \frac{9265}{T} + 0.0051\left(\frac{P-1}{T}\right),$$

(Huebner and Sato, 1970).

Preliminary experiments were carried out on the Mn_2O_3-Mn_3O_4 buffering mixture to investigate the limits of its effectiveness with time at varying temperatures. At 850°C and 1000 bars the buffering mixture was largely converted to Mn_3O_4 after about 4 days; at 800°C, 6 days were required for complete conversion, and at 700°C some 9 days. At 600°C the buffering assemblage appeared virtually unchanged after 14 days.[2] For experiments whose run time exceeded the buffering capacity at the particular temperature, the run was interrupted and the charge reconstituted with fresh buffering material. Some corrosion of Ag/Pd capsules by manganese oxides was observed although this was not a serious problem. Pt capsules were found suitable for some higher temperature runs. Iron loss to Pt was probably negligible at high f_{O_2} levels, and no discrepancies were noticed between results from using one or the other capsule material.

The phase relations were obtained largely from synthesis experiments using the gel starting materials. H_2O contents of gels were determined to be in the region of 2–3 wt percent and so the amount of water added to charges (no more than 5 percent) was kept low to minimize vapor-phase leaching effects. However, even under melting conditions an aqueous vapor-phase was invariably present, as indicated by small amounts of an amorphous quench product. Glass quenched from liquid is red-brown to colorless, and is distinguishable (with some difficulty) from the amorphous quench material. Needles tentatively identified as sodium metasilicate by X-ray diffraction were sometimes noticed among the latter. Due to vapor-leaching, it must be assumed that the total of condensed-phase compositions from any run is never exactly equivalent to the bulk composition of the starting material, although it would appear that this effect is of less importance in acmite-rich portions of the system.

For accurate determination of the pyroxene solidi, previous run products from the hyper-solidus regions were re-run at consecutively lower temperatures. The cell parameters of pyroxenes formed as exclusive single phases (occasionally plus negligible hematite) are in reasonable accord (see Table 3) with pyroxenes synthesized directly from gels.

Phases were determined optically and by X-ray powder diffraction. Pyroxene cell parameters were determined from X-ray diffraction patterns by a least-squares refinement of 2θ measurements using a computer program modified from that of Burnham (1962). The region from 70° to 5° 2θ was scanned at 1/4° per minute, using Ni-filtered Cu radiation. Twelve peaks were measured by reference to an internal silicon standard and indexed by comparison with the pattern given by Nolan and Edgar (1963) for pure acmite.

Crystalline Phases

(1) Acmitic pyroxenes crystallized in the system Na_2O-Fe_2O_3-Al_2O_3-TiO_2-SiO_2 at the Mn_2O_3-Mn_3O_4 buffer are pale ruddy-brown. Well-formed prismatic or acicular crystals, up to 100μ in length, exhibit the pleochroism: X, yellow-brown; Y, straw-yellow; and Z, foxy-brown. Pyroxenes crystallized at the Ni-NiO and Fe_3O_4-Fe_2O_3 buffers are pale green, suggesting the presence of Fe^{2+} ions. Refractive indices are comparable to those given by Nolan (1969) and Yagi (1966).

(2) Hematite forms as small but highly conspicuous hexagonal crystals up to 50μ across that are dark red-brown in plane polarized light and blood-red under crossed nicols.

(3) Freudenbergite, a sodium-iron titanate belonging to the solid-solution series $Na_2O \cdot Fe_2O_3 \cdot (6 + x)TiO_2$, occurs as subhedral prisms up to about 100μ in length. It shows straight extinction and has refractive indices (of about 1.51) that are substantially lower than average pyroxene values. Depending on the thickness of crystals, it varies from straw-yellow to ruddy-brown in color and shows faint pleochroism. Its presence was initially confirmed from its unique X-ray pattern (McKie, 1966) and optical properties, which differ slightly from those of the isostructural sodium-titanate series (Wadsley, 1964; Bayer and Hoffmann, 1965, 1966).

(4) Pseudobrookite is yellow to reddish-brown and is faintly pleochroic. It was only observed in the presence of glass and of the phases nepheline, hematite, and freudenbergite, but never with pyroxene. It is easily identifiable from its high refractive indices, birefringence, and very strong dispersion.

(5) Nepheline appears as small prismatic crystallites of characteristically low birefringence. From the X-ray diffraction pattern, the 27.290° $2\theta_{(21\bar{3}0)}$ and 29.795°

[2] There was no evidence that the outer capsule burst during these runs.

$2\theta_{(20\bar{2}2)}$ peaks (Cu$K\alpha$ radiation) for nepheline formed in the 'four-phase' region pyroxene + hematite (?) + nepheline + freudenbergite show significant shifts from the values (27.240° and 29.690°) for pure synthetic nepheline. These shifts probably indicate solid solution towards an iron-nepheline molecule ($NaFe^{3+}SiO_4$). Incorporation of excess SiO_2 in the nepheline structure is a further possibility (Hamilton and MacKenzie, 1960; Bailey and Schairer, 1966).

Experimental Results

(1) *The Join $NaFe^{3+}Si_2O_6$-$NaTiFe^{3+}SiO_6$ (Acmite-tf)*

This join proceeds from acmite composition towards the silica-poor part of the four-component Na_2O-Fe_2O_3-TiO_2-SiO_2 system and, if extended, intersects the silica-free 'basal' plane Na_2O-Fe_2O_3-TiO_2 at composition $Na_2O \cdot Fe_2O_3 \cdot 4TiO_2$; (see Figs. 1 and 2). The experimental results are presented in Table 1, and the isobaric phase diagram for 1000 bars P_{H_2O} is given in Figure 3.

At temperatures less than about 700°C, crystallization of gel starting materials was sluggish, and, except for the acmite end-member itself, there was no direct confirmation that equilibrium had been reached, even for runs of several weeks. The solid-line phase boundaries in Figure 3 have been confirmed by experiments employing products and synthesized phase assemblages of previous runs as starting materials (see below). These results (Table 1) are not at variance with those from synthesis experiments, and a close approach to equilibrium may be assumed for runs above 700°C. Charges from runs on $ac_{80}tf_{20}$ (900°C), $ac_{70}tf_{30}$ (800°C) and $ac_{60}tf_{40}$ (800°C) were each held at consecutively lower temperatures (see Table 1), and from the disappearance of hematite it was possible to locate the solidus and part of the solvus curves.

The melting temperature for pure acmite at the Mn_2O_3-Mn_3O_4 buffer is greater than 900°C, which is at least 10°C higher than that indicated by Bailey (1969) and confirmed by the present author at the Fe_3O_4-Fe_2O_3 buffer at 1000 bars. This may be taken as a probable maximum for crystallization in nature in the presence of excess H_2O, because introduction of Fe^{2+} would reduce the melting temperature. At the 700°C isotherm, binary solid solution of the tf component in acmite exists up to about 28 mole percent. At more tf-rich compositions, an undefined but small interval of ternary solid solution exists, where pyroxene$_{ss}$ coexists with freudenbergite only,

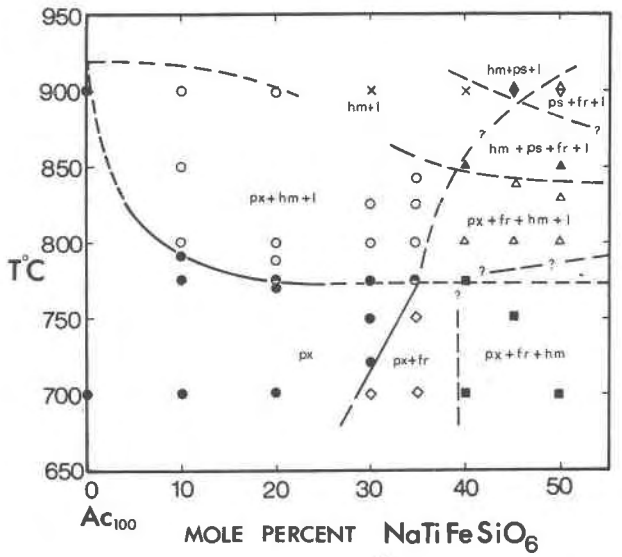

FIG. 3. Schematic phase relations for part of the join acmite-tf at 1000 bars total water pressure. Symbols as follows: px, pyroxene solid solution; hm, hematite; fr, freudenbergite solid solution; ps, pseudobrookite; and l, liquid (glass).

succeeded by the association, pyroxene$_{ss}$ + freudenbergite + hematite. Despite our imprecise knowledge of both pyroxene and freudenbergite solid solutions, it is unlikely that each pair of compositions lies with hematite in the same triangular plane as the respective bulk compositions (see Fig. 1). The implied fourth phase is not present, unless we assume it to be a sodium silicate that remains largely dissolved in the vapor phase on quenching of the charge.

The composition $NaFeTiSiO_6$ (tf) may be represented by equal mole proportions of $Na_2Ti_2Si_2O_9$ (ramsayite) and Fe_2O_3 (hematite); hence three compositions on the join ramsayite-hematite—namely, at $rams_{90}hm_{10}$, $rams_{80}hm_{20}$, and $rams_{50}hm_{50}$ (tf)—were made using synthetic ramsayite and hematite. The resulting phase assemblage from runs on $rams_{50}hm_{50}$ at 1000 bars P_{H_2O} and in the temperature range 650°–770°C is identical to that from gel composition tf_{100} under these conditions: *viz* pyroxene$_{ss}$ + freudenbergite + hematite (plus amorphous quench), ramsayite having entirely disappeared. However, run products from $rams_{90}hm_{10}$ and $rams_{80}hm_{20}$ contained ramsayite + pyroxene$_{ss}$ + freudenbergite in differing proportions, and ramsayite itself has been synthesized without difficulty from a gel of composition $Na_2Ti_2Si_2O_9$ (Flower, in preparation). Further experiments carried out on $ac_{70}tf_{30}$ and $ac_{50}tf_{50}$, made up from synthetic acmite, ramsayite, and hematite resulted in the breakdown of ramsayite, and confirmed

the narrow two-phase field of pyroxene$_{ss}$ + freudenbergite (Fig. 3). The assemblage pyroxene$_{ss}$ + freudenbergite + hematite (+ Na = silicate ?) is also confirmed as the exclusive subsolidus assemblage for titanium-rich parts of the join.

The solidus-liquidus region is more complicated. The most titanium-rich pyroxene solid solutions begin melting incongruently at 775°C (±10) to hematite + liquid and, within an interval of 80–100°C, react completely to hematite + pseudobrookite + freudenbergite + liquid. This region has not been studied in detail as it is largely beyond the temperature range of the hydrothermal equipment, although a brief study was made of the 900° isotherm using the internally heated gas-media apparatus. Results from these experiments show that pseudobrookite, coexisting with liquid ± hematite and/or freudenbergite, probably has a wide field of stability at high temperatures for the more titanium-rich compositions. Pseudobrookite is clearly not stable below a certain (as yet undefined) temperature in this join, and probably shows a reaction relation with tf-rich pyroxene solid solutions.

At the high ambient f_{O_2}, hematite probably shows minimal solid solution towards titanium-bearing species (*cf* Haggerty, 1970); thus it would follow that, below the temperature of pseudobrookite stability, titanium would be largely partitioned between pyroxene, freudenbergite, and the liquid phase. If the pyroxene solid solution essentially involves the acmite and tf molecules, the freudenbergite must be richer in both Na_2O and TiO_2 but poorer in Fe_2O_3, as compared to the composition of natural freudenbergite (Fig. 1) given by Frenzel (1961).

Experiments on compositions $ac_{90}tf_{10}$, $ac_{70}tf_{30}$, $ac_{50}tf_{50}$ and tf_{100} buffered by the Ni-NiO assemblage (Table 1) indicate that pyroxene miscibility is considerably restricted relative to that at the Mn_2O_3-Mn_3O_4 buffer. The melting point of 'acmite' was measured to be 830°C (±10) at the Ni-NiO buffer, some 20°C less than that measured by Nolan (1966). The coexistence of ilmenite ($Fe^{2+}TiO_3$) with pryoxene and freudenbergite for composition $ac_{70}tf_{30}$ at subsolidus temperatures, together with the restricted extent of pyroxene cell parameter variation (Fig. 5), suggests that miscibility is no greater than about 18 mole percent tf in acmite. Solid solution at lower f_{O_2} is almost certainly more complex than at the Mn_2O_3-Mn_3O_4 buffer and may involve the molecules $Na_2Fe^{2+}Ti^{4+}Si_4O_{12}$ or $NaTi^{3+}Si_2O_6$ (Prewitt, Shannon, and White, 1972).

(2) *The Join $NaFe^{3+}Si_2O_6$-$NaTiAlSiO_6$ (Acmite-tx)*

Within the pseudoquaternary system, $NaFeSiO_4$-$NaAlSiO_4$-TiO_2-SiO_2 (Fig. 2), the acmite-tx join lies within the triangular join acmite-TiO_2-$NaAlSiO_4$, because tx is equivalent to equal mole proportions of nepheline and rutile. It appears that aluminum, with titanium, is able to enter the acmitic pyroxene structure as the tx molecule. The experimental results for the acmite-tx join are given in Table 2, and the isobar phase diagram at 1000 bars is shown in Figure 4. Binary solid solution of tx in acmite at the Mn_2O_3-Mn_3O_4 buffer extends up to about 15 mole percent at 700°C; more tx-rich bulk compositions result in pyroxene solid solutions (possibly toward tf) accompanied by nepheline. In this two-phase field, a silica-rich phase (*e.g.*, albite) might be expected, although none is actually encountered. It must be assumed that silica and Na_2O are taken up by the vapor phase, although nepheline may take some SiO_2 and Fe_2O_3 in solid solution. At more tx-rich compositions, pyroxene and nepheline coexist with freudenbergite and hematite. The presence of hematite, as for the acmite-tf join where hematite is almost without doubt a subsolidus phase for tf-rich bulk compositions, may be a consequence of the vapor-leaching, but this has not been unequivocally confirmed. In any case, with or without hematite, pyroxene$_{ss}$ + freudenbergite + nepheline comprise the subsolidus between compositions richer in tx than

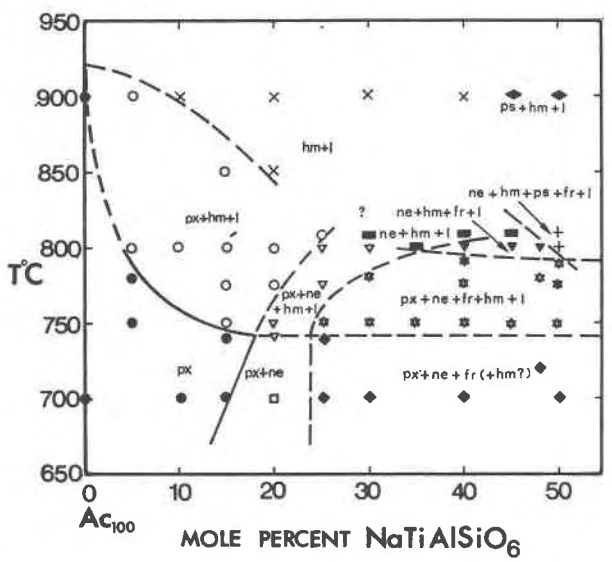

FIG. 4. Schematic phase relations for part of the join acmite-tx at 1000 bars total water pressure. Symbols same as in Figure 3 with the addition of ne, nepheline.

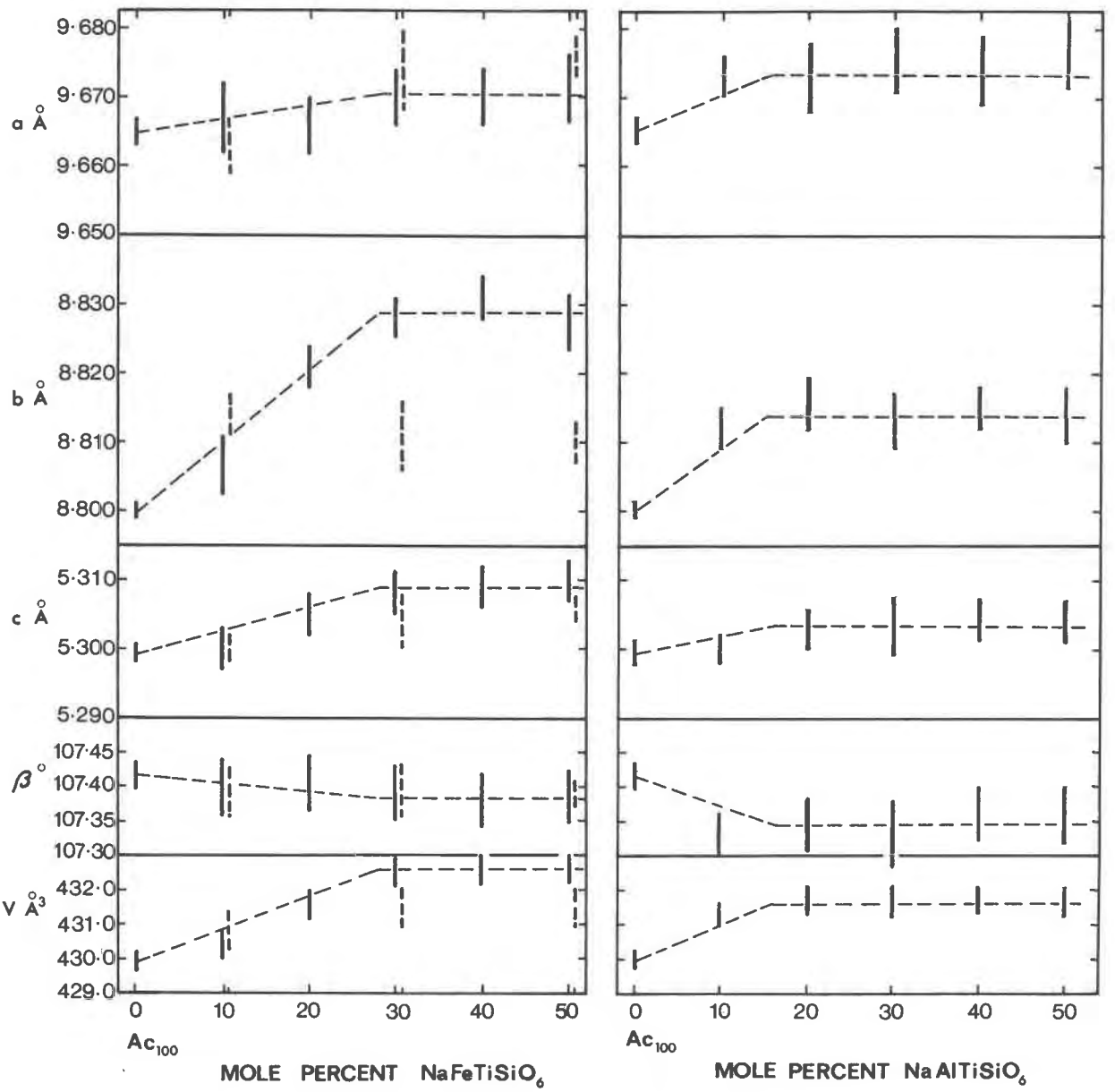

FIG. 5. Variation of cell parameters a, b, c, β and V of pyroxenes formed from bulk compositions along the joins acmite-tf and acmite-tx. All data are presented in Table 3, where coexisting phases are indicated for non-binary parts of each join. Solid lines are for pyroxenes formed at the Mn_2O_3–Mn_3O_4 buffer, and dashed lines for those formed at the Ni–NiO buffer.

about 24 mole percent and an as yet undefined point where rutile is stable. The composition tx crystallizes as nepheline + rutile only, at all subsolidus temperatures and over a wide pressure range. No information is available for the region between $ac_{30}tx_{70}$ and tx_{100}.

To verify the stable coexistence of subsolidus phases within this join, the compositions $ac_{70}tx_{30}$, $ac_{80}tx_{20}$, and $ac_{50}tx_{50}$ were made up from the pure synthetic end-member phases acmite, nepheline, and rutile. In spite of thorough grinding of starting materials, the rutile proved relatively unreactive. For $ac_{50}tx_{50}$ it required a month at 700°C and 1000 bars for complete disappearance of rutile and recrystallization to pyroxene + nepheline + freudenbergite + hematite (+ a trace of Na-silicate). Leakage reduced the $ac_{70}tx_{30}$ after one month and, although rutile had disappeared, pyroxene$_{ss}$ coexisted with nepheline, ilmenite, freudenbergite, and nepheline. The $ac_{80}tx_{20}$

charge run under the same conditions reacted to produce pyroxene$_{ss}$ + nepheline (see Table 2).

The interval for complete reaction of the most tx-rich solid solutions is ~120°C, substantially more than that for exclusively tf-rich pyroxenes. In other parts of the join, phase relations are very complex, particularly in view of vapor-phase leaching effects, and the interpretations in Figure 4 are approximations. Investigations of the 900°C isotherm using the internally heated vessel (Table 2) indicate the widespread occurrence of pseudobrookite coexisting with nepheline + hematite + liquid, with nepheline + hematite + freudenbergite + liquid, or with hematite + freudenbergite + liquid. Incompatibility of pseudobrookite with pyroxene was again evident. Pseudobrookite is clearly unstable below 790°C (±10), some 200°C above its lower breakdown temperature in the system FeO-Fe_2O_3-TiO_2 (Haggerty and Lindsley, 1970; Haggerty, 1970). It is again of interest to note the persistence of freudenbergite to relatively high temperatures in the five-component system.

(3) Cell Parameter Variation in Pyroxene Solid Solutions

The lattice parameters a, b, c, β and V have been determined for pyroxenes crystallized at 10 mole percent intervals from acmite to 50 percent tf and tx, including pyroxenes formed in non-binary parts of the joins. The data (Table 3) are plotted against bulk composition of charges in Figure 5. There is reasonable correspondence between data for pyroxenes synthesized from gel starting materials and those formed from crystalline assemblages of the same bulk composition (Table 3). Compared to the overall variation, the standard deviation is rather large and must be attributed to inaccuracies introduced by the poor crystallinity of the material. Scanning the sample more than two times at 1/4° per minute did not noticeably contribute to a better cell refinement. However, entry of the tf molecule into acmite seems to increase the unit cell volume (V) and parameters a, b, and c, while decreasing the angle β. A similar effect is observed for inclusion of tx. There is no conclusive indication of the nature of ternary solid solution that exists in the two phase (pyroxene$_{ss}$ + nepheline) field.

Due to the poor crystallinity of the pyroxenes, optical data are not available for the most titanium-rich members. Variation of the cell data, however, does give a fairly exact indication of the miscibility limits in the two joins, provided none of the solid solution is metastable. The restricted miscibility at the Ni-NiO buffer is also apparent from cell data for acmite-tf pyroxenes (Fig. 5).

For solid solutions between acmite and tf pyroxene, the increase in cell volume is attributed to the need for either Ti^{4+} (ionic radius = 0.680 Å[3]), or Fe^{3+} (0.645 Å) to substitute for Si^{4+} (0.42 Å) in the tetrahedral-site, while substitution of Ti^{4+} for Fe^{3+} would additionally increase the a and b cell edges. In tx-bearing pyroxenes, entry of Al^{3+} (0.530 Å) into tetrahedral sites would also expand the cell volume, in contrast to Al^{3+} entry into octahedral sites as observed in acmite-jadeite pyroxenes (Popp and Gilbert, 1972), where cell volumes are reduced. The overall variation of cell data therefore is assumed to reflect the coupled substitutions FeSi = TiFe and FeSi = TiAl in tf- and tx-bearing pyroxenes respectively. Hartman (1969) has argued convincingly against tetrahedral coordination of Ti^{4+} as a general rule. Al^{3+} and Fe^{3+} (in that order) would seem more likely candidates.

Petrogenetic Applications

Phase Relations

The experimental data presented above define the extent of titanium and aluminum substitution in acmitic pyroxenes in terms of the molecules $NaFeTiSiO_6$ and $NaAlTiSiO_6$. Phase relations in the investigated region of the Na_2O-Fe_2O_3-Al_2O_3-TiO_2-SiO_2 system are of most interest with respect to peralkaline igneous rocks—peralkalinity defined as the ratio (Na + K)/Al exceeding unity—in which acmite is the most significant pyroxene component. Peralkaline rocks are frequently associated with high oxidation levels during their genesis (Bailey and Schairer, 1966), and the Mn_2O_3-Mn_3O_4 buffer is believed to be an appropriate upper f_{O_2} boundary for their experimental study.

From the present investigation it is important to note (1) the fairly extensive pyroxene miscibility in this system, (2) the stable coexistence of the phases pyroxene$_{ss}$ + freudenbergite + hematite with liquid (plus an aqueous vapor phase) in the more titanium-rich parts of the acmite-tf join, and (3) these phases plus nepheline in the acmite-tx join. In both joins pseudobrookite is stable only at temperatures above that at which pyroxene disappears.

[3] All ionic radii quoted in this paper are the values from Shannon and Prewitt (1969) for octahedrally-coordinated ions.

Titanium and Aluminum Contents of Natural Acmite

Acmitic pyroxene (aegirine) is rarely observed as primary phenocrysts in lavas, ignimbrites, *etc.* Petrographic evidence suggests that it forms as a late-stage component, often mantling earlier-formed aegirine-augite in the groundmass, rather than as a reaction product formed between magma and previously-crystallized iron-titanium oxides (see Nolan, 1966). Many, but not all, of such late-stage pyroxenes are moderately titaniferous, although there is scant indication from 'whole crystal' analyses that titanium content is related to the proportion of acmite present.

Detailed electron microprobe studies on lavas from Tenerife (Scott, 1970), and ignimbrites from Gran Canaria (Schmincke and Frisch, in preparation) have shown an enrichment of up to ~25 mole percent tf in outer zones of groundmass aegirine. This approaches the experimental miscibility limit at the Mn_2O_3-Mn_3O_4 buffer (Fig. 3). The relative extent of Ti-enrichment is illustrated in Figure 6, where atomic proportions of Ti^{4+} are plotted against Na^+ for several contrasting pyroxene series. In outer calcium-free zones of titan-aegirines from Gran Canaria, titanium content is almost double that of typical zoned titan-augites from Tenerife (Scott, 1970), while soda-augites and aegirine-augites of intermediate soda content are conspicuously low in titanium. Titan-aegirine has also been reported from the Katzenbuckel (Odenwald) by Freudenberg (1919) with a whole-crystal TiO_2 content of 5.88 wt percent.

The Canaries sodic pyroxenes are from rock types that are typical products of protracted magmatic fractionation, and their strong zonation and enrichment in tf (and in the Tenerife aegirines, tx), may suggest this to be a more widespread phenomenon than whole-crystal aegirine analyses and CIPW norm recalculations would otherwise suggest. In alkaline complexes such as the Lovozero Intrusion (Kola Peninsula), metasomatic introduction of soda and silica may be an important factor in the formation of Na-titanates and Na-Ti-silicates by reaction with oxides under conditions of high f_{O_2}. Late-stage aegirines in alkaline rocks are frequently yellow-brown in color and may themselves be significantly titaniferous (*e.g.*, Katzenbuckel), although few analytical data, particularly for compositional zoning, are available. For less oxidized intrusions such as the Qoroq nepheline-syenite in South Greenland (Stephenson, 1972), pyroxene data do not indicate any late-stage titanium enrichment (Fig. 6), and tend to suggest that titanium is more exclusively contained in oxide minerals. Aluminum contents of volcanic and plutonic aegirines are hardly significant when compared to the high contents of the soda-poor (calcic) pyroxenes of basic and intermediate rocks (Fig. 7). There is a slight indication of relative aluminum enrichment with increasing Na^+ in pyroxenes from Itapirapua (Gomes, Moro, and Datra, 1970) and Tenerife (Scott, 1970), both from thoroughly undersaturated rock series. Positive correlation of aluminum and titanium in the Tenerife aegirines suggests incorporation of the tx molecule (up to ~8 mole percent), while the high aluminum and low titanium in the Itapirapua pyroxenes (Gomes *et al*, 1970) probably reflects solid solution towards a jadeitic end-member.

TABLE 3. Cell Parameters of Pyroxenes*

Charge Compn.	Coexisting Phases	a(Å)	b(Å)	c(Å)	β°	V(Å³)
Oxygen Buffer: Mn_2O_3-Mn_3O_4; 700°C ± 10; Starting material: gel						
ac_{100}	none	9.665(2)	8.800(1)	5.299(1)	107.42(2)	430.0(2)
tf_{10}	none	9.667(5)	8.807(4)	5.299(3)	107.40(4)	430.4(4)
tf_{20}	none	9.666(4)	8.821(3)	5.305(3)	107.41(4)	431.6(4)
tf_{30}	none	9.670(4)	8.828(3)	5.308(3)	107.39(4)	432.5(4)
tf_{40}	fr+hm	9.670(4)	8.831(3)	5.309(3)	107.38(4)	432.7(4)
tf_{50}	fr+hm	9.672(5)	8.827(4)	5.310(3)	107.39(4)	432.6(4)
tx_{10}	none	9.673(3)	8.812(3)	5.300(2)	107.33(3)	431.3(3)
tx_{20}	ne	9.673(5)	8.817(4)	5.303(3)	107.34(4)	431.7(4)
tx_{30}	ne+fr+(hm)	9.676(5)	8.813(4)	5.303(2)	107.33(5)	431.7(5)
tx_{40}	ne+fr+hm+?	9.674(5)	8.815(3)	5.304(3)	107.36(4)	431.7(4)
tx_{50}	ne+fr+hm+?	9.673(5)	8.814(4)	5.304(3)	107.36(4)	431.7(4)
Oxygen Buffer: Ni-NiO; 700°C ± 10; Starting material: gel						
tf_{10}	ilm	9.663(4)	8.814(3)	5.300(2)	107.39(4)	430.8(4)
tf_{30}	fr+ilm	9.674(6)	8.811(5)	5.304(4)	107.39(5)	431.5(6)
tf_{50}	fr+ilm	9.676(3)	8.810(3)	5.306(2)	107.41(2)	431.5(3)
Oxygen Buffer: Mn_2O_3-Mn_3O_4; 750°C ± 10; Starting material: px+hm+gl						
tx_5	none	9.669(5)	8.810(4)	5.300(4)	107.38(5)	430.9(5)
Oxygen Buffer: Mn_2O_3-Mn_3O_4; 750°C ± 10; Starting material: ac+ne+ru						
tx_{20}	ne	9.667(3)	8.808(3)	5.299(2)	107.36(3)	430.6(3)

*Cell parameters shown with one standard error (in parentheses) in terms of last decimal cited, thus 9.665(2) indicates a standard error of ±0.002.

Natural Occurrence of Freudenbergite

Natural freudenbergite has been found in nepheline-syenites from the Katzenbuckel (Frenzel, 1961) commonly accompanied by zoned aegirine and hematite. The appearance elsewhere in Katzenbuckel rocks of both hematite and pseudobrookite testifies to the high ambient f_{O_2} during their late-stage crystallization and/or alteration, while groundmass aegirine and aegirine-augite crystals are rimmed with titan-acmite (Frenzel, personal communication, 1972). The occurrence of freudenbergite intergrown with hematite

—$(010)_{fr}$ parallel to $(0001)_{hm}$, Frenzel (1961)—may conceivably reflect a reaction relationship not yet detected from experimental work, although it more probably results from reaction during cooling of titan-acmite (Fig. 3). The natural freudenbergite corresponds to the formula $Na_2Fe_2Ti_7O_{18}$ (Frenzel, 1961), although it is known to be a non-stoichiometric member of the series $Na_2O \cdot Fe_2O_3(6 + x)TiO_2$ with a unit cell based on 16 oxygen atoms (Bayer and Hoffmann, 1965; McKie and Long, 1970). There is also strong evidence from the present work and that of Bayer and Hoffmann of solid solution towards the structurally related sodium-titanate 'bronzes' (*e.g.*, $Na_{0.2}TiO_2$) reported by Anderson and Wadsley (1962).

Factors Governing Titanium and Aluminum Partition

The main factor inhibiting aluminum uptake by aegirine in nature is clearly its preferential incorporation by feldspars in bulk magma compositions where there is an excess of sodium, potassium, and calcium over the Fe^{3+} and Ti^{4+} available for pyroxene formation. Depletion of aluminum in magma by plagioclase and alkali feldspar fractionation is the major prerequisite for acmite to form at all (see Bailey and Schairer, 1966), although more aluminum would be available if the approach to peralkalinity were to result in a relatively greater removal of CaO, K_2O, and SiO_2. In a thoroughly undersaturated (*e.g.*, ijolitic) melt, any remaining aluminum would be partitioned between pyroxene and nepheline. Aluminum entry into the tetrahedral sites of pyroxene would be facilitated by entry of Ti^{4+} into the octahedral *M*1 site, if Ti^{4+} is not preferentially combined in oxides.

Entry of titanium into acmite, at least as tf (but probably also as tx) is clearly favored by high temperature (Figs. 3, 4). Another factor affecting miscibility is silica activity. From comparison with the miscibility of jadeite in acmite at low pressure (4 kbar) on the join $NaFeSi_3O_8$-$NaAlSi_3O_8$ (Popp and Gilbert, 1972), solid solution of tx allows relatively more

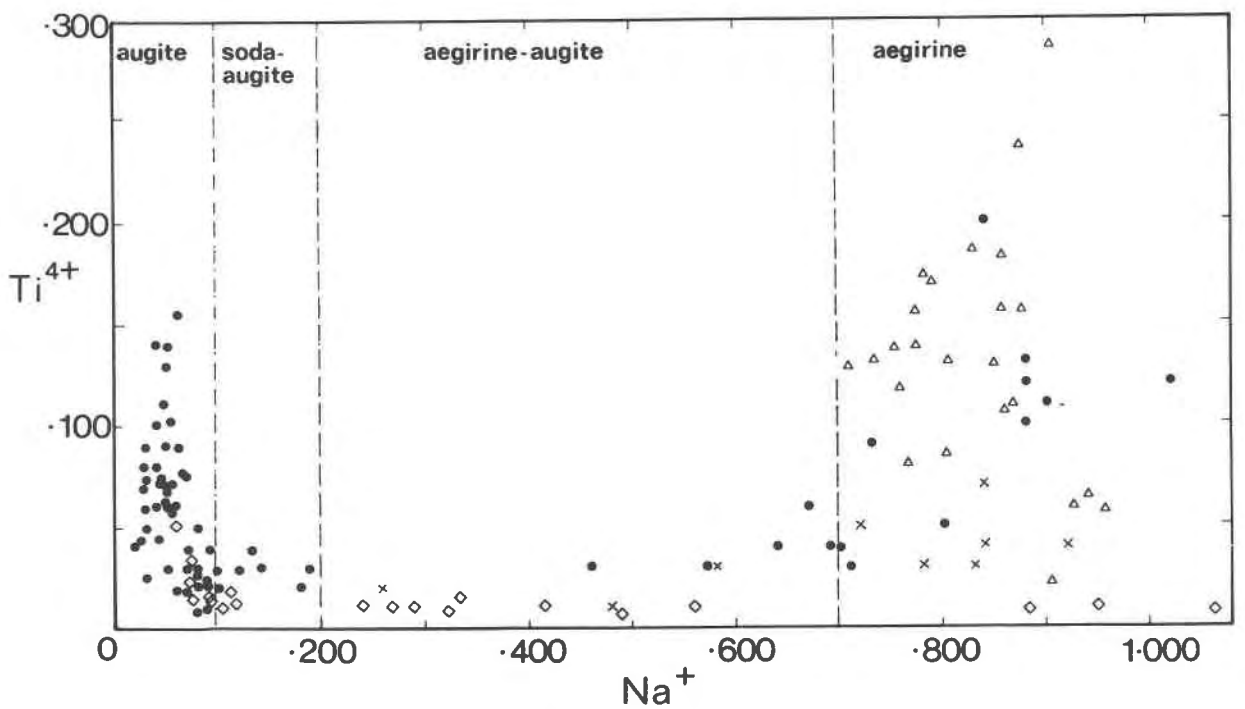

FIG. 6. Plots of Ti^{4+} versus Na^+ (cations per 6 oxygens) for contrasting series of pyroxenes.
The symbols used represent:
●, augite-aegirine pyroxene series from undersaturated lavas of Las Canadas Volcano, Tenerife (Scott, 1970);
△, aegirines (whole-crystal and individual zone analyses) from Miocene ignimbrite flow, Gran Canaria (Schmincke and Frisch, in preparation);
◇, augite-aegirine pyroxene series (selected data) from the Qoroq nepheline-syenite intrusion, south Greenland (Stephenson, 1972);
×, aegirine-augites and aegirines from East African fenites (Sutherland, 1969).

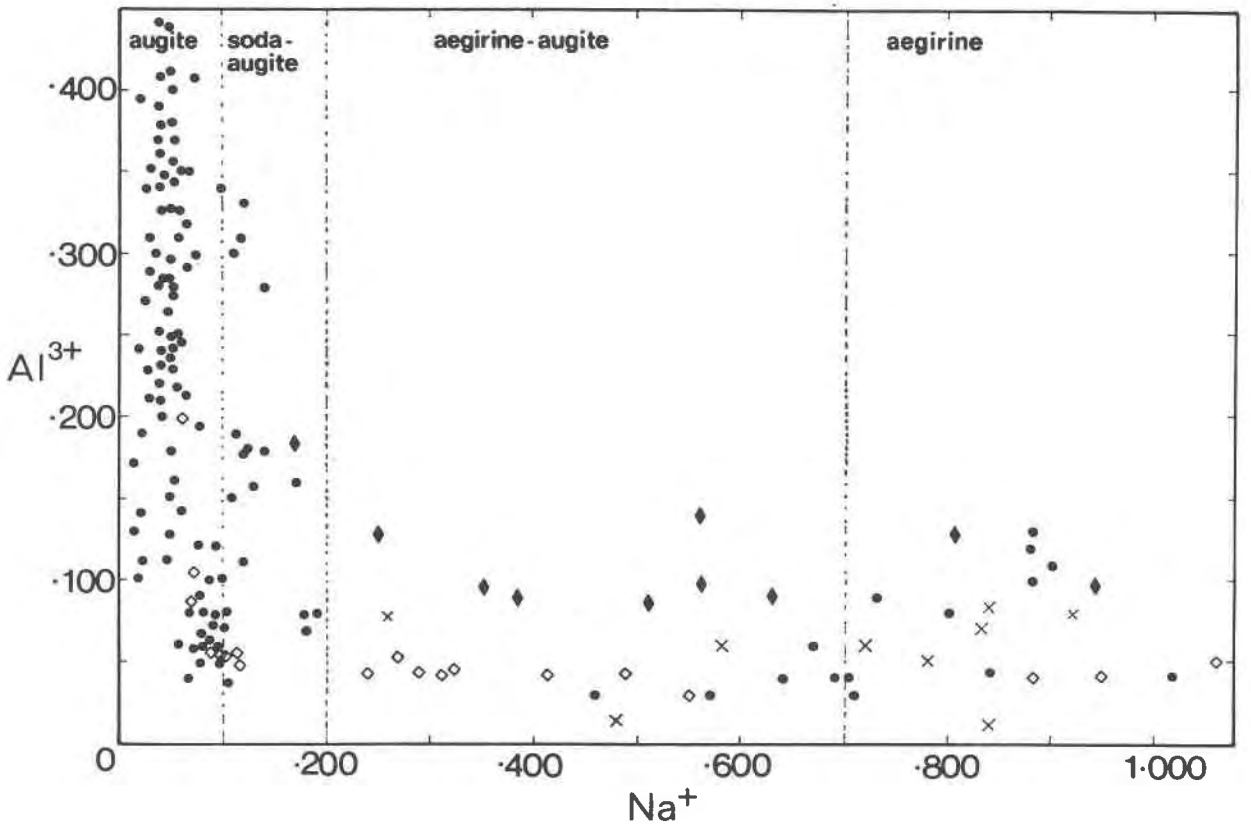

FIG. 7. Plots of Al^{3+} versus Na^{+} (cations per 6 oxygens) for contrasting series of pyroxenes. Symbols: as for Figure 6 but more data for augites are included. The black diamonds indicate aegirine-augites and aegirines from nepheline-syenite intrusion, Itapirapua, Brazil, (Gomes, Moro, and Dutra, 1970).

aluminum (and hence titanium) to enter acmite, suggesting that low silica activity promotes easier entry of aluminum into tetrahedral sites. However, the most important (indirect) influence on titanium entry is the oxygen fugacity. High contents of acmite in natural pyroxene are taken to denote relatively oxidized conditions compared to other common iron-bearing pyroxenes, although Bailey (1969) and also Ernst (1962) showed experimentally its stable persistence under surprisingly reduced conditions, *e.g.*, at the Fe_3O_4-FeO buffer. The present work indicates that Ti^{4+} entry would be facilitated by the scarcity of Fe^{2+}-bearing species at high f_{O_2}, which may otherwise preferentially enter and stabilize acmite at lower f_{O_2} levels. The data from natural titan-aegirines show a general positive correlation of Ti^{4+} with tetrahedrally assigned Fe^{3+} (Schmincke and Frisch, in preparation) while a strong negative correlation of Ti^{4+} with octahedrally assigned $Fe^{3+} + Mn^{2+} + Mg^{2+}$ (Schmincke and Frisch, in preparation) is a clear indication of Ti entry into *M*1 octahedral sites, Al^{3+} being assigned to the tetrahedra.

Acknowledgments

The writer extends thanks to Professor W. Schreyer for initiating the project, and to Dr. M. C. Gilbert and Professors F, Seifert and H.-U. Schmincke for critically reading the manuscript. F. Seifert is also thanked for conducting the experiments in the internally-heated apparatus, and Dr. K. Langer for help with the chemical analysis and preparation of the gels.

References

ANDERSON, S., AND A. D. WADSLEY (1962) $Na_xTi_4O_8$, an alkali metal titanium bronze. *Acta Crystallogr.* **15,** 201–206.

AOKI, K. (1959) Petrology of alkalic rocks of the Iki Islands and Higashi-Matsura district, Japan. *Tohoku Univ. Sci. Rep. 3rd Ser.* **6,** 261–310.

——— (1964) Clinopyroxenes from alkaline rocks of Japan. *Am. Mineral.* **49,** 1199–1223.

BAILEY, D. K. (1969) The stability of acmite in the presence of water. *Am. J. Sci.* **267-A,** 1–16.

———, AND J. F. SCHAIRER (1966) The system Na_2O-Al_2O_3-Fe_2O_3-SiO_2 at one atmosphere, and the petrogenesis of alkaline rocks. *J. Petrol.* **7,** 114–170.

BARTH, T. F. W. (1931) Pyroxen von Hiva Oa, Marquesas-Inseln, und die Formel titan-haltigen Augite. *Neues Jahrb. Mineral.* **64,** 217–224.

BAYER, G., AND W. HOFFMANN (1965) Uber Verbindungen vom Na_xTiO_2-Typ. *Z. Kristallogr.* **121,** 9–13.

———, AND ——— (1966) Oxydverbindungen mit Na_xTiO_2-Struktur, und deren Bedeutung fur das Freudenbergit Problem. *Fortschr. Mineral.* **42,** 203.

BURNHAM, C. W. (1962) Lattice constant refinement. *Carnegie Inst. Washington Year Book,* **61,** 132–135.

CARMICHAEL, I. S. E. (1962) Pantelleritic liquids and their phenocrysts. *Mineral. Mag.* **33,** 86–113.

CASSIE, R. M. (1970) The melting behavior of diopside-acmite pyroxenes at high pressures. *Carnegie Inst. Washington Year Book,* **69,** 170–175.

ERNST, W. G. (1962) Synthesis, stability, and occurrence of riebeckite and riebeckite-arfvedsonite solid solutions. *J. Geol.* **70,** 689–736.

EUGSTER, H. P., AND D. R. WONES (1962) Stability relations of the ferruginous biotite, annite. *J. Petrol.* **3,** 82–125.

FRENZEL, G. (1961) Ein neues Mineral: Freudenbergit ($Na_2Fe_2Ti_7O_{16}$). *Neues Jahrb. Mineral. Monatsh.* **1,** 12–22.

———, J. OTTEMANN, AND B. NUBER (1971) Neue Mikrosonden-Untersuchungen an Freudenbergiten. *Neues Jahrb. Mineral. Mh.* **12,** 547–551.

FREUDENBERG, W. (1919) Titanbiotit (Wodanit) vom Katzenbuckel, nebst Bemerkungen uber Sanidin, Aegirin, Apatit, und Granat vom gleichen Fundort. *Mitt. Badisch. Geol. Landesanst.* **8,** 319–340.

GILBERT, M. C. (1967) X-ray properties of jadeite-acmite pyroxenes. *Carnegie Inst. Washington Year Book,* **66,** 374–375.

——— (1969) High pressure stability of acmite. *Am. J. Sci.* **267-A,** 145–159.

GOMES, C DE B., S. L. MORO, AND C. V. DUTRA (1970) Pyroxenes from the alkaline rocks of Itapirapua, Sao Paulo, Brazil. *Am. Mineral.* **55,** 224–230.

GORDON, S. G. (1924) Minerals obtained in Greenland on the second Academy-Vaux expedition, 1923. *Acad. Nat. Sci. Philadelphia Proc.* **76,** 249–268.

HAGGERTY, S. E. (1970) High-temperature oxidation of ilmenite in basalts. *Carnegie Inst. Washington Year Book,* **70,** 165–176.

———, AND D. H. LINDSLEY (1970) Stability of the pseudobrookite (Fe_2TiO_5)-ferropseudobrookite ($FeTi_2O_5$) series. *Carnegie Inst. Washington Year Book,* **68,** 247–249.

HAMILTON, D. L., AND C. M. B. HENDERSON (1968) The preparation of silicate compositions by a gelling method. *Mineral. Mag.* **36,** 832–838.

———, AND W. S. MACKENZIE (1960) Nepheline solid solution in the system $NaAlSiO_4$-$KAlSiO_4$-SiO_2. *J. Petrol.* **1,** 56–72.

HARTMAN, P. (1969) Can Ti^{4+} replace Si^{4+} in silicates? *Mineral. Mag.* **37,** 366–369.

HUCKENHOLZ, H. G. (1969) Synthesis and stability of Ti-andradite. *Am. J. Sci.* **267-A,** 209–232.

HUEBNER, J. S., AND M. SATO (1970) The oxygen fugacity-temperature relationships of manganese oxide and nickel oxide buffers. *Am. Mineral.* **55,** 934–952.

KUSHIRO, I. (1964) Petrology of the Atumi dolerite, Japan. *Tokyo Fac. Sci. J.* **15,** 135–202.

LINDSLEY, D. H., AND S. E. HAGGERTY (1970) Phase relations of iron-titanium oxides and aenigmatite; oxygen fugacity of pegmatoid zones. *Carnegie Inst. Washington Year Book,* **69,** 278–284.

MCKIE, D. (1963) The unit-cell of freudenbergite. *Z. Kristallogr.* **132,** 157–169.

———, AND J. V. P. LONG (1970) The unit-cell contents of freudenbergite. *Z. Kristallogr.* **132,** 157–160.

NOLAN, J. (1966) Melting relations in the system $NaAlSi_3O_8$-$NaAlSiO_4$-$NaFeSi_2O_6$-$CaMgSi_2O_6$-H_2O and their bearing on the genesis of alkaline undersaturated rocks. *Quart. J. Geol. Soc. London,* **122,** 119–157.

——— (1969) Physical properties of synthetic and natural pyroxenes in the system diopside-hedenbergite-acmite. *Mineral. Mag.* **36,** 5–21.

———, AND A. D. EDGAR (1963) An X-ray investigation of synthetic pyroxenes in the system acmite-diopside-water at 1000 kg/cm^3 water vapour pressure. *Mineral. Mag.* **33,** 625–634.

POPP, R. K., AND M. C. GILBERT (1972) Stability of acmite-jadeite pyroxenes at low pressure. *Am. Mineral.* **57,** 1210–1231.

PREWITT, C. T., R. D. SHANNON, AND W. B. WHITE (1972) Synthesis of a pyroxene containing trivalent titanium. *Contrib. Mineral. Petrol.* **35,** 77–82.

SCHMINCKE, H-U. (1969) Ignimbrite sequence on Gran Canaria. *Bull. Volcanol.* **33,** 1199–1219.

SHANNON, R. D., AND H. C. PREWITT (1969) Effective ionic radii in oxides and fluorides. *Acta Crystallogr.* **B-25,** 925–946.

SCOTT, P. (1970) *Mineralogy of Lavas from Tenerife, Canary Islands.* Ph.D. thesis, Imperial College, University of London.

STEPHENSON, D. (1972) Alkali clinopyroxenes from nepheline-syenites of the South Qoroq centre, south Greenland. *Lithos,* **5,** 187–201.

SUTHERLAND, D. S. (1969) Sodic amphiboles and pyroxenes from fenites in East Africa. *Contrib. Mineral. Petrol.* **24,** 114–135.

TIBA, T. (1966) Petrology of the alkaline rocks of the Takakusayama district, Japan. *Tohuku Univ. Sci. Rep.* **9,** 541–610.

VERHOOGEN, J. (1962) Distribution of titanium between silicates and oxides in igneous rocks. *Am. J. Sci.* **260,** 211–220.

WADSLEY, A. D. (1964) The possible identity of freudenbergite and Na_xTiO_2. *Z. Kristallogr.* **120,** 396–398.

YAGI, K. (1953) Petrochemical studies on the alkalic rocks of the Morotu district, Sakhalin. *Geol. Soc. Am. Bull.* **64,** 769–810.

——— (1966) The system acmite-diopside and its bearing on the stability relations of natural pyroxenes of the acmite-hedenbergite-diopside series. *Am. Mineral.* **51,** 976–1000.

———, AND K. ONUMA (1967) The system $CaMgSi_2O_6$-$CaTiAl_2O_6$ and its bearing on the titan-augites. *Hokkaido Univ. Fac. Sci. J.* **13,** 463–483.

YODER, H. S. (1950) High-low quartz inversion up to 10000 bars. *Am. Geophys. Union Trans.* **31,** 827–835.

Manuscript received, May 17, 1973; accepted for publication, November 29, 1973.